



A new chaotic jerk system with a sinusoidal nonlinearity, its bifurcation analysis, multistability, circuit design and complete synchronization design via backstepping control

Sundarapandian VAIDYANATHAN , Fareh HANNACHI , Irene M. MOROZ ,
Chittineni ARUNA , Mohamad Afendee MOHAMED  and Aceng SAMBAS 

In this research work, we investigate a new three-dimensional jerk system with three parameters in which one of the nonlinear terms is a sinusoidal nonlinearity. We show that the new jerk system has two unstable equilibrium points on the x -axis. Numerical integrations show the existence of periodic and chaotic states, as well as unbounded solutions. Consideration of the Poincaré sphere at infinity found no periodic states. We show that the new jerk system exhibits multistability with coexisting attractors. We also present results for the offset boosting of the proposed chaotic jerk system. Using MultiSim version 14.1, we design an electronic circuit for the new jerk system with a sinusoidal nonlinearity. As a control application, we design complete synchronization for the master-slave jerk systems using backstepping control technique. Simulations are presented to illustrate the main results of this research work.

Copyright © 2024. The Author(s). This is an open-access article distributed under the terms of the Creative Commons Attribution-NonCommercial-NoDerivatives License (CC BY-NC-ND 4.0 <https://creativecommons.org/licenses/by-nc-nd/4.0/>), which permits use, distribution, and reproduction in any medium, provided that the article is properly cited, the use is non-commercial, and no modifications or adaptations are made

S. Vaidyanathan (corresponding author, e-mail: sundarytu@gmail.com) is with Centre for Control Systems, Vel Tech University, 400 Feet Outer Ring Road, Avadi, Chennai-600062 Tamil Nadu, India and Faculty of Information and Computing, Universiti Sultan Zainal Abidin Terengganu, Malaysia.

F. Hannachi (e-mail: fareh.hannachi@univ-tebessa.dz) is with Larbi Tebessi University – Tebessi, route de constantine, 12022, Tebessa, Algeria.

I.M. Moroz (e-mail: Irene.Moroz@maths.ox.ac.uk) is with Mathematical Institute, University of Oxford, Andrew Wiles Building, ROQ, Oxford OX2 6GG, UK.

C. Aruna (e-mail: aruna.cse@kitsguntur.ac.in) is with Department of Computer Science and Engineering, KKR & KSR Institute of Technology and Sciences, Vinjanampadu, Vatticherukuru Mandal, Guntur-522017, Andhra Pradesh, India.

M.A. Mohamed (e-mail: mahendee@unisza.edu.my) is with Faculty of Information and Computing, Universiti Sultan Zainal Abidin, Terengganu, Malaysia.

A. Sambas (e-mails: acengsambas@unisza.edu.my, acengs@umtas.ac.id) is with Faculty of Informatics and Computing, Universiti Sultan Zainal Abidin, Gong Badak, 21300, Terengganu, Malaysia and Department of Mechanical Engineering, Universitas Muhammadiyah Tasikmalaya, Jawa Barat 46196, Indonesia.

Received 16.10.2023. Revised 7.02.2024.

Key words: chaos, chaotic systems, jerk systems, mechanical systems, bifurcation analysis, backstepping control, synchronization, circuit design

1. Introduction

Chaotic systems are nonlinear dynamical systems which are characterized by the presence of at least one positive Lyapunov exponent indicating high sensitivity to small changes in the initial conditions for the dynamical systems [1, 2]. Chaotic systems are applied in many engineering areas such as encryption [3, 4], memristive systems [5, 6], communication systems [7, 8], robotics [9, 10], finance systems [11, 12], etc.

A mechanical jerk system is a third order differential equation given as

$$\ddot{x} = J(x, \dot{x}, \ddot{x}), \quad (1)$$

where J is a globally continuously differentiable mapping.

Using the signal variables $y = \dot{x}$ and $z = \ddot{x}$, we can express the jerk differential equation (1) in the system form as follows:

$$\begin{cases} \dot{x} = y, \\ \dot{y} = z, \\ \dot{z} = J(x, y, z). \end{cases} \quad (2)$$

For mechanical differential equations, $x(t)$ represents the displacement, $y(t) = \dot{x}(t)$ represents the velocity and $z(t) = \ddot{x}(t)$ represents the acceleration of the mechanical body under consideration. In such cases, $\ddot{x}(t)$ represents the jerk of the mechanical body. This is the physical interpretation for the jerk mechanical differential equations.

Jerk systems exhibiting chaotic behavior have many applications in science and engineering [13, 14]. Li and Zeng [15] discussed the multi-scroll attractor and multi-stable dynamics of a 3-D chaotic jerk system. Xia *et al.* [16] derived new results for a chaotic bursting attractor for a controlled jerk oscillator. Vaidyanathan *et al.* [17] detailed the modelling of a new multistable chaotic jerk system with two unstable equilibrium points and discussed the field programmable gate array (FPGA) design of the proposed jerk system. Zourmba *et al.* [18] discussed the modelling of a new chaotic oscillator with diode-inductor nonlinear bipole-based jerk circuit.

In this paper, we propose a new chaotic jerk system having a sinusoidal nonlinearity and three quadratic nonlinearities. We show that the new jerk system has two unstable equilibrium points on the x -axis. We conduct a detailed bifurcation analysis of the proposed jerk system. It is well-known that bifurcation

analysis is carried out to extract useful dynamical properties of dynamical systems [19,20]. Next, we show that the proposed jerk system exhibits multistability with coexisting attractors. Multistability of chaotic systems has many engineering applications [21,22].

Offset boosting is an important issue for chaos control due to its broadband property and polarity control [23,24]. We also explore the offset boosting control properties for the new chaotic system. For practical applications, circuit designs of chaotic systems will be very useful [25,26]. Using MultiSim 14.1, we build an electronic circuit for the proposed jerk system.

Finally, we give a control application of the proposed jerk system, *viz.* complete synchronization of a pair of proposed jerk systems considered as *master* and *slave* systems. Synchronization of chaotic systems has applications in engineering areas such as secure communications [27,28]. We use backstepping control method for the synchronization design of the master-slave chaotic jerk systems. Backstepping is a powerful control technique that allows the design of a feedback control law for a special class of nonlinear systems such as systems having a recursive structure that guarantees the stability of the system [29,30]. Since the jerk systems possess a triangular structure, backstepping control method is often applied by control engineers for control and synchronization of jerk systems [13,28].

2. Mathematical model of the new jerk system

In this section, we detail the mathematical model of a new jerk system with four nonlinear terms. The new jerk system is described as follows:

$$\begin{cases} \dot{x} = y, \\ \dot{y} = z, \\ \dot{z} = -ax - b \sin x - cx^2 + y^2 - xy - z. \end{cases} \quad (3)$$

We remark that the new jerk system (3) possesses three quadratic nonlinearities and a sinusoidal nonlinearity in its dynamics. Also, a , b , and c are system parameters which are assumed to take positive values. We shall establish using an analysis with Lyapunov exponents that the new jerk system (3) is chaotic.

We take the parameter values as $a = 1.6$, $b = 0.2$ and $c = 0.2$. Then the Lyapunov exponents of the jerk system (3) can be calculated for the initial state $(0.5, 0.2, 0.5)$ as follows:

$$\tau_1 = 0.16067, \quad \tau_2 = 0, \quad \tau_3 = -1.16067. \quad (4)$$

Since the Lyapunov Exponents (LE) spectrum given in (4) have the sign pattern $(+, 0, -)$, and the total values equal to -1 , which is negative, we conclude that

the jerk system (3) has a chaotic attractor and that the system is dissipative. Furthermore, the Kaplan-Yorke dimension of the new jerk system (3) is determined as follows:

$$D_{KY} = 2 + \frac{\tau_1 + \tau_2}{|\tau_3|} = 2.1384. \tag{5}$$

The Kaplan-Yorke dimension of a chaotic system indicates the complexity of the system [31].

Next, the equilibrium points of the jerk system (3) are calculated by means of following the system of equations:

$$y = 0, \tag{6a}$$

$$z = 0, \tag{6b}$$

$$-ax - b \sin x - cx^2 + y^2 - xy - z = 0. \tag{6c}$$

From (6a) and (6b), we find that $y = z = 0$.

Substituting the values $y = 0$ and $z = 0$ in (6c), we obtain

$$ax + b \sin x + cx^2 = 0. \tag{7}$$

For the chaotic case, $a = 1.6$, $b = 0.2$ and $c = 0.2$. Then the equation (7) becomes

$$1.6x + 0.2 \sin x + 0.2x^2 = 0 \quad \text{or} \quad x^2 + 8x + \sin x = 0 \tag{8}$$

which has two roots $x = 0$ and $x = -8.1189$.

Thus, the jerk system (3) has two equilibrium points described by

$$P_0 = \begin{bmatrix} 0 \\ 0 \\ 0 \end{bmatrix} \quad \text{and} \quad P_1 = \begin{bmatrix} -8.1189 \\ 0 \\ 0 \end{bmatrix}. \tag{9}$$

The eigenvalues of the Jacobian matrix for the jerk system (3) at P_0 are found as

$$\alpha_1 = -1.6552, \quad \alpha_{2,3} = 0.3281 \pm 0.9895i \tag{10}$$

which shows that the equilibrium point P_0 is a saddle-focus and unstable.

The eigenvalues of the Jacobian matrix for the jerk system (3) at P_1 are found as

$$\alpha_1 = -3.3025, \quad \alpha_2 = -0.2053, \quad \alpha_3 = 2.5078 \tag{11}$$

which shows that the equilibrium point P_1 is a saddle-point and unstable.

Thus, we have shown that the new jerk system (3) has two unstable equilibrium points P_0 and P_1 on the x -axis.

Figure 1 depicts the 2-D and 3-D MATLAB plots of the chaotic attractor of the new jerk system (3) for the initial state $(0.5, 0.2, 0.5)$ and the parameter vector $(a, b, c) = (1.6, 0.2, 0.2)$.

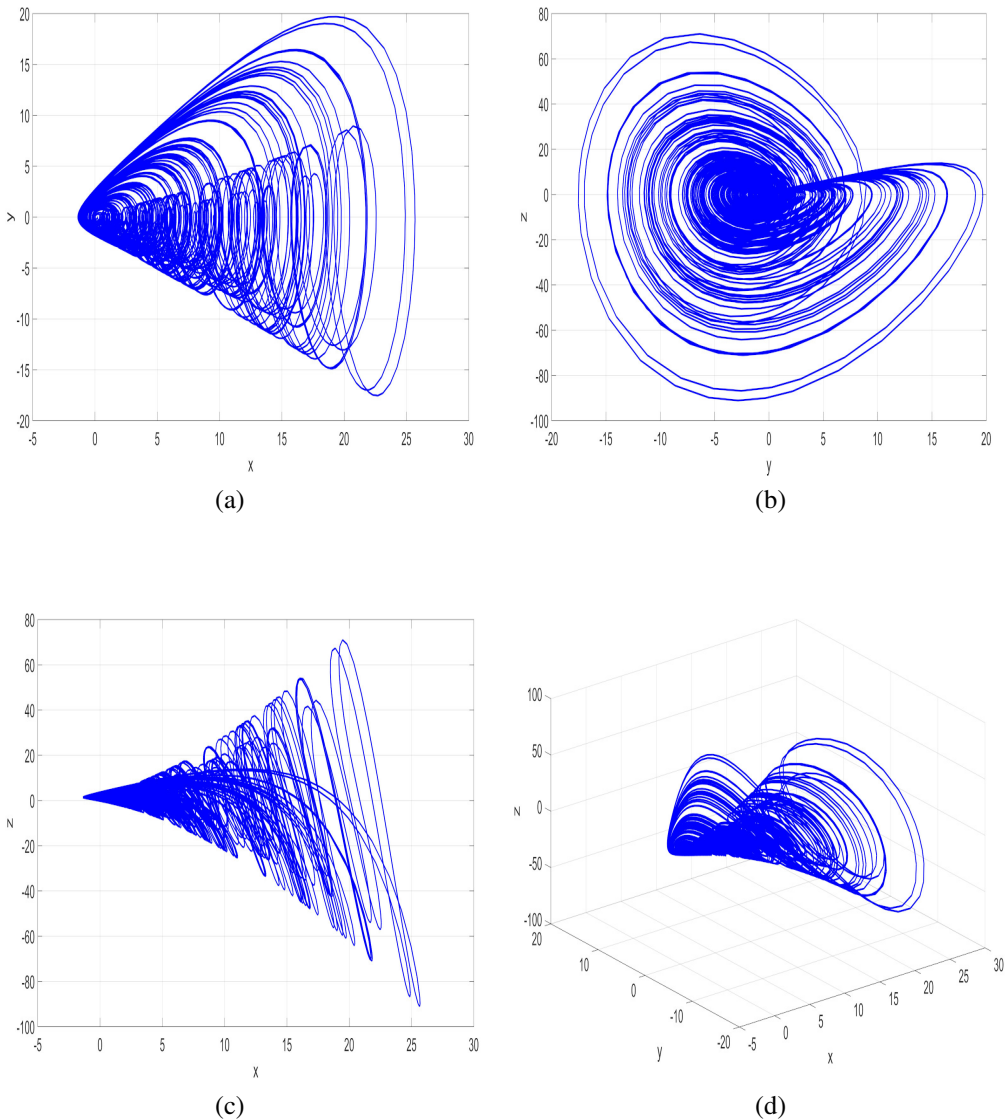


Figure 1: 2-D and 3-D plots of the chaotic attractor of the new jerk system (3) for the initial state $(0.5, 0.2, 0.5)$ and the parameter vector $(a, b, c) = (1.6, 0.2, 0.2)$

3. Bifurcation analysis of the new jerk system

The new three-dimensional jerk system is

$$\begin{cases} \dot{x} = y, \\ \dot{y} = z, \\ \dot{z} = -ax - b \sin x - z - cx^2 - xy + y^2. \end{cases} \tag{12}$$

Although the chosen set of parameter values is $(a, b, c) = (1.6, 0.2, 0.2)$, it is of interest to explore the dynamics of (12) for other values of these parameter values. We do this by finding bifurcation transition plots as each parameter varies in turn. We also plot the fixed points and their linear stabilities as functions of each parameter.

There is a trivial fixed point, found by setting the RHS of (12) to zero to get $\mathbf{x}_0 = (x, y, z)_0 = (0, 0, 0)$. There is also a nontrivial fixed point $\mathbf{x}_e = (x_e, 0, 0)$, where $x = x_e$ satisfies the equation $ax + b \sin x + cx^2 = 0$. Figure 2 shows the locus of fixed points as a , b and c vary in turn.

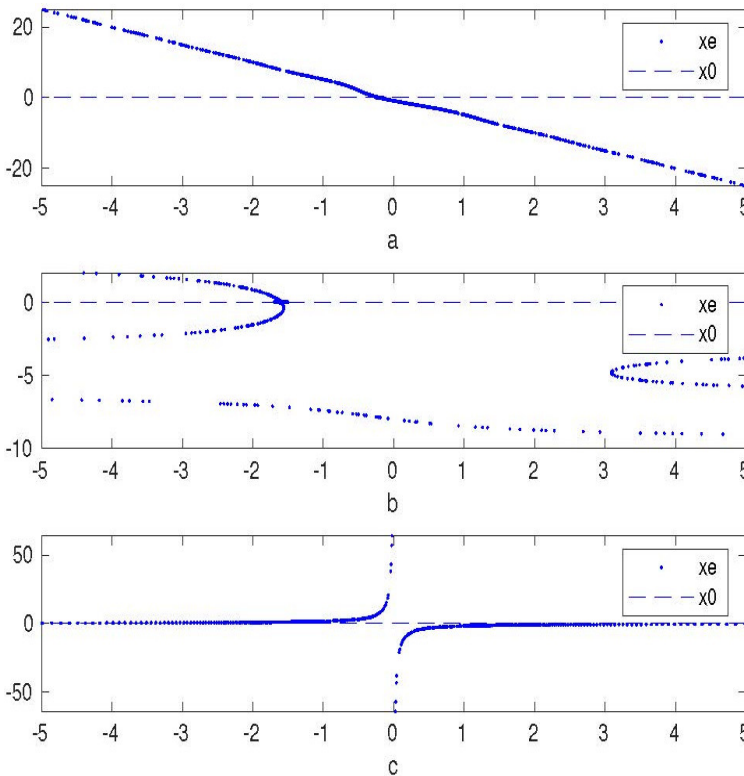


Figure 2: The fixed points for the trivial (- -) and nontrivial (. .) fixed points as (a) a varies, (b) b varies and (c) c varies

The linear stability of each fixed point is determined from the characteristic polynomial. We first compute the Jacobian matrix:

$$J = \begin{pmatrix} 0 & 1 & 0 \\ 0 & 0 & 1 \\ -(a + b \cos x + 2cx + y) & 2y - x & -1 \end{pmatrix}. \tag{13}$$

The characteristic equation is the determinant of $J - \lambda I_3$, evaluated at each fixed point where λ denote the eigenvalues and I_3 is the (3, 3) identity matrix.

(i) For \mathbf{x}_0 , we obtain the cubic characteristic equation:

$$\lambda^3 + \lambda^2 + a + b = 0. \tag{14}$$

(ii) For \mathbf{x}_e , we obtain the characteristic equation:

$$\lambda^3 + \lambda^2 + \lambda x_e + (a + b \cos(x_e) + 2cx_e) = 0. \tag{15}$$

Figure 3 shows the linear eigenspectra for both the trivial and nontrivial fixed points for $-5 \leq a \leq 5$ for $b = 0.2$ and $c = 0.2$. For the chosen set of parameter

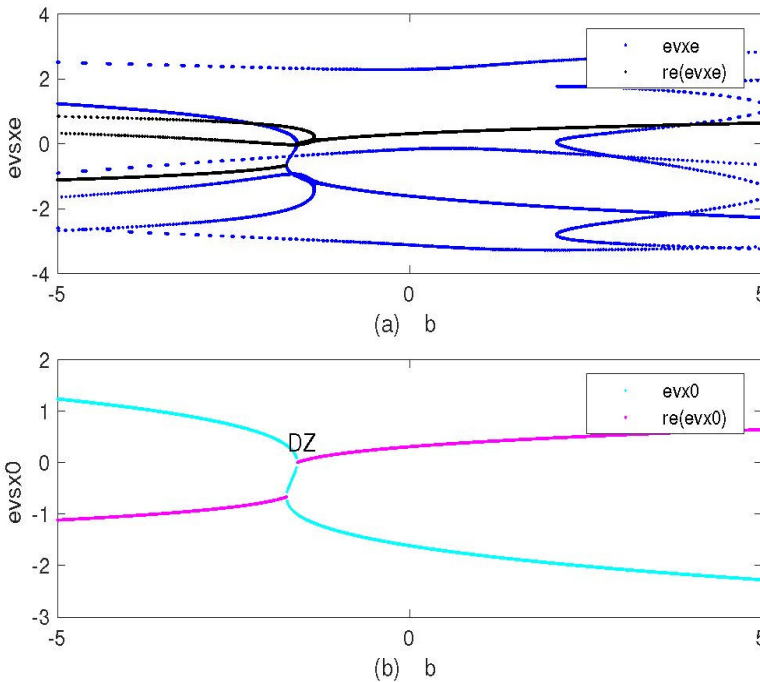


Figure 3: The linear eigenspectra for (a) the nontrivial and (b) the trivial equilibrium states for $-5 \leq a \leq 5$ and $b = 0.2, c = 0.2$. The blue curve tracks the real eigenvalue and the black curve tracks the real part of the complex eigenvalues for the nontrivial equilibrium state. The cyan curve tracks the real eigenvalue and the magenta curve tracks the real part of the complex eigenvalue for the trivial equilibrium state

values ($a = 1.6$), both fixed points are unstable. The trivial fixed point is unstable throughout, whereas the nontrivial fixed point is stable for $a < -0.25$. Figure 2(b) shows that the locus of fixed points x_e crosses the dashed line of $x_0 = 0$ when $b = -a = -1.6$. This corresponds to a double zero eigenvalue for both eqns (14) and (15). There is also a turning point in the x_e plot when $b \approx -1.56$, and when $b \approx 3.09$. Inspection of the constant coefficient of the characteristic equation (15) gives the former as a zero eigenvalue for x_e .

3.1. Numerical Integrations

Figure 4 shows the bifurcation transition plot for x_{\max} as a varies for $0.13 \leq a \leq 1.7$. We see there are windows of periodic and chaotic states. For $a > 0.17$, the trajectories became unbounded. We also integrated the system for $a < 0$ and found steady state solutions for $a < -0.205$. For example, for $a = -0.225$, we obtained the steady state $x_e \approx 0.1277$. When $a = -0.2$, the trajectories diverged to infinity. We were unable to find the presence of a Hopf bifurcation.

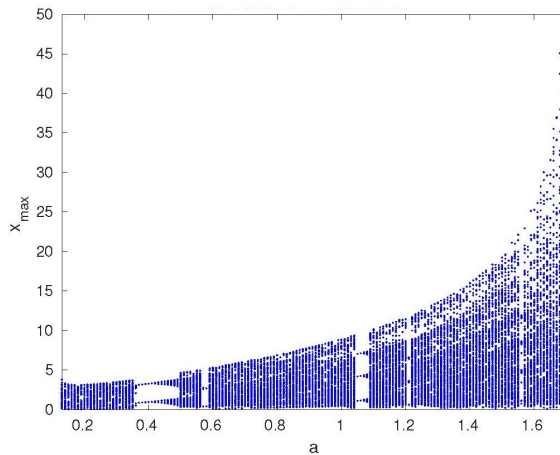


Figure 4: The bifurcation transition plots of x_{\max} as a varies for $0.13 \leq a \leq 1.7$, initial conditions $\mathbf{x}_i = (0.5, 0.2, 0.5)$

Figure 5 shows the corresponding bifurcation transition plot for x_{\max} as b varies. Now there are bounded state for $-1.5 \leq b \leq 0.29$, with a larger range of periodic solutions. Finally Figure 6 shows the bifurcation transition plot as c varies. Again we find bounded states for a range of $0.07 \leq c \leq 0.73$, but unbounded solutions outside this range.

These figures show chaotic dynamics for the chosen set of parameter values.

We also investigated the Poincaré sphere at infinity to see if we could find stable states, but we found only unbounded states.

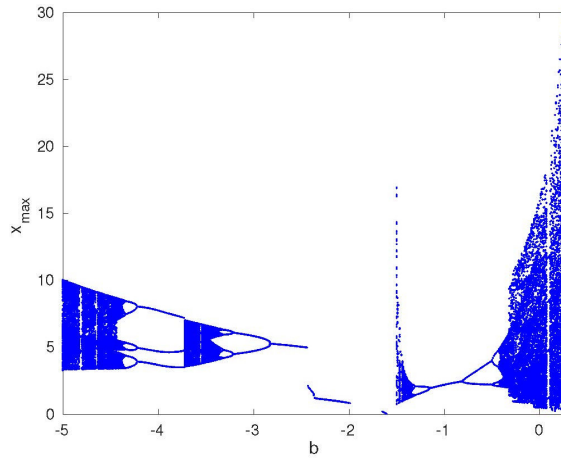


Figure 5: The bifurcation transition plots of x_{\max} as b varies for $-5 \leq b \leq 0.29$, initial conditions $\mathbf{x}_i = (0.5, 0.2, 0.5)$

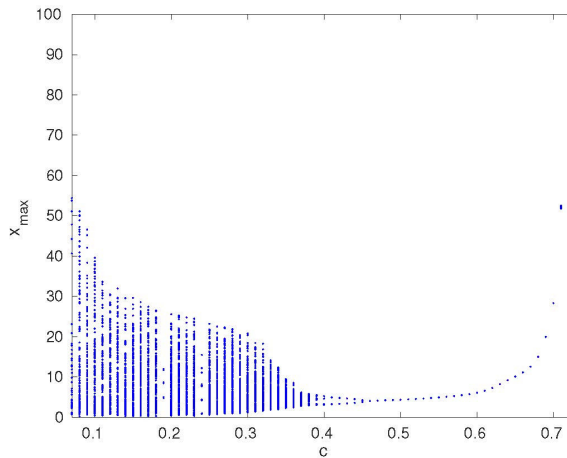


Figure 6: The bifurcation transition plots of x_{\max} as c varies for $0.07 \leq c \leq 0.73$, initial conditions $\mathbf{x}_i = (0.5, 0.2, 0.5)$

3.2. Discussion of the bifurcation analysis results

We investigated the dynamics of the new 3-D jerk system for a range of parameter values as all three parameters vary in turn. The linear stability analysis for both equilibrium states shows that the characteristic equations (14) and (15) become identical when $x_e = 0$, leading to a degenerate double-zero bifurcation when, in addition, $a + b = 0$.

Numerical integrations show the existence of bounded periodic and chaotic solutions, as well as unbounded states. This is particularly evident in the bifur-

cation transition plot of x_{\max} vs b of Figure 5. Unbounded solutions are found for $b > 0.29$ and $-1.6 < b < -1.5$. There is then a second range of bounded periodic and chaotic states, before we find unbounded states for $b < -8$.

4. Multistability in the new 3-D chaotic jerk system

In order to study the coexistence attractors and other characteristics of the jerk system (3) better, it is necessary to give some disturbance to the initial conditions under the condition of keeping the system parameters constant. Figures 7 and 8 show the dynamic behavior with coexistence chaotic attractors with different initial conditions.

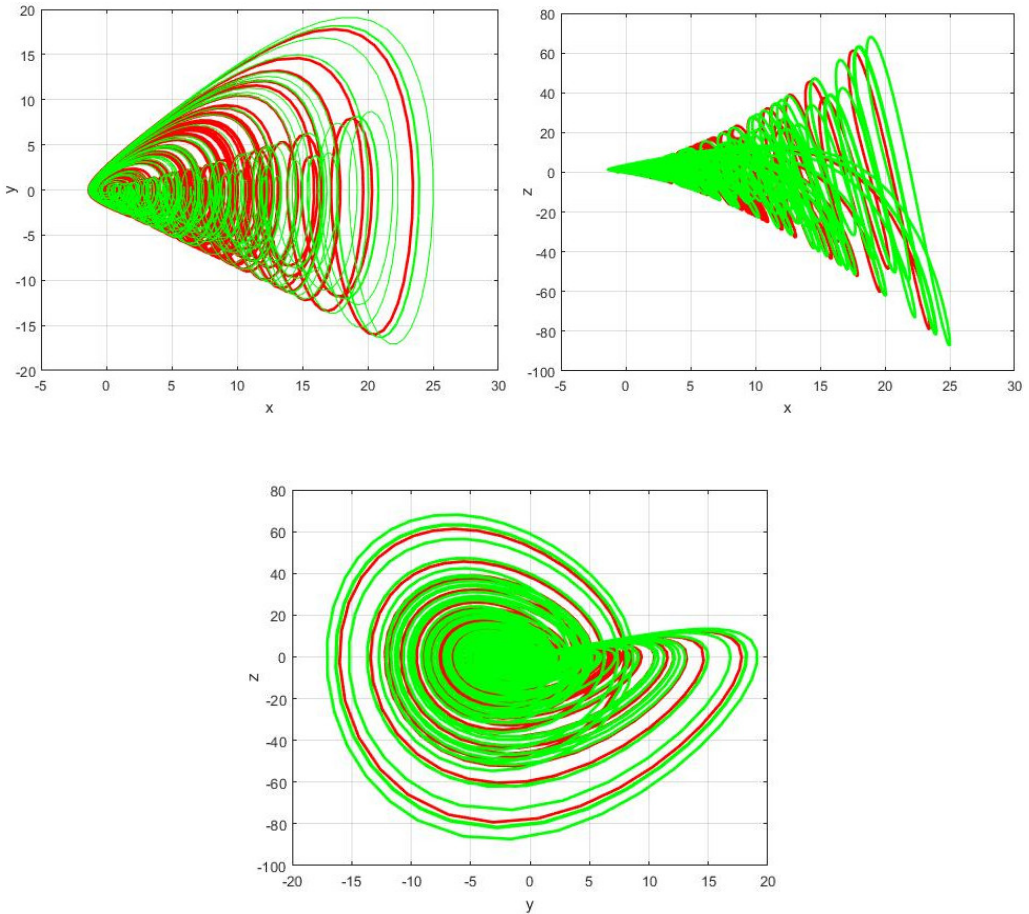
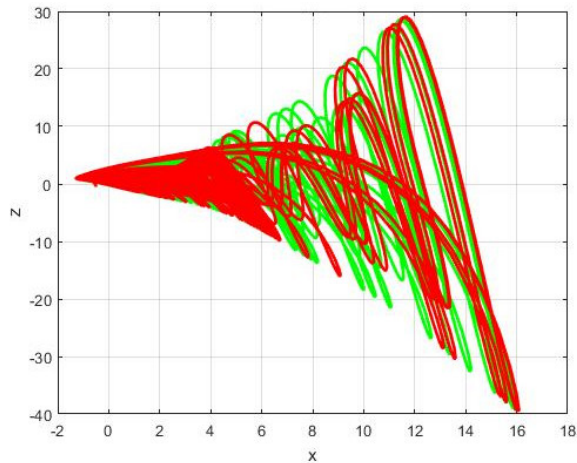
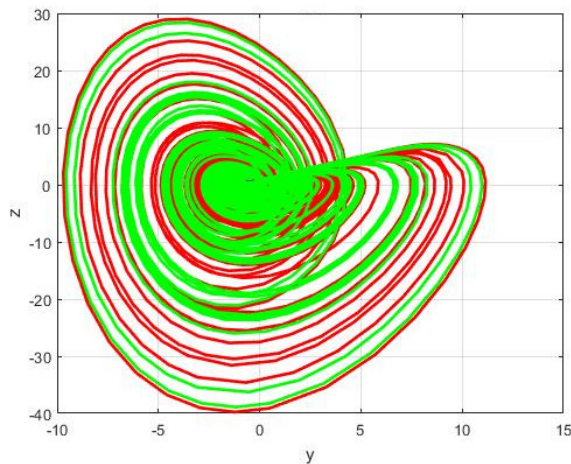


Figure 7: Coexistence of two attractors of the jerk system (3) with different initial values: the red for $(0.5, 0.2, 0.5)$ and the green for $(-0.5, -0.2, -0.5)$



(a)



(b)

Figure 8: Coexistence of two chaotic attractors of the jerk system (3) for the parameters: $a = 0.6$, $b = 1$, $c = 0.2$ and with different initial conditions: (a) the red for $(1, 0, 1)$ and the green for $(5, 2, 1)$, (b) the red for $(0.5, 0.2, 0.5)$ and the green for $(-0.5, 0, -0.5)$

5. Offset boosting for the new 3-D chaotic jerk system

In this section, we will discuss the offset boosting control. Adding a constant m to a variable in a nonlinear system (3) will produce an offset. Obviously, the state of the jerk system (3) can be controlled and the offset-boosted system is obtained from the jerk system (3) by replacing a state variable ξ with $\xi + m$ in the equations of the jerk system (3) as follows:

Case1: for z variable

The system (1) can be controllable and the offset-boosted system is obtained from system (1) by replacing z with $z + m$ in the equations of the system (3) as follows:

$$\begin{cases} \dot{x} = y, \\ \dot{y} = z + m, \\ \dot{z} = -ax - b \sin x - c(x)^2 - xy + (y)^2 - (z + m). \end{cases} \quad (16)$$

It can be seen from Figure 9 that signal z can be transformed from a bipolar signal to a bipolar signal when varying the control parameter m .

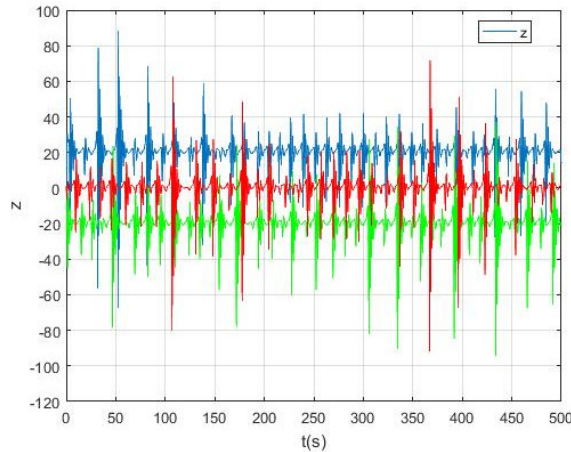


Figure 9: The signal z of the system (16) with different values of the offset boosting controller m : for $m = -20$ (blue colour); $m = 0$ (red colour); $m = 20$ (green colour)

Case2: for x variable

The jerk system (3) can be controlled and the offset-boosted system is obtained from the system (3) by replacing x with $x + m$ in the third equation of the jerk system (3) as follows:

$$\begin{cases} \dot{x} = y, \\ \dot{y} = z, \\ \dot{z} = -a(x + m) - b \sin(x + m) - c(x + m)^2 - (x + m)y + (y)^2 - z. \end{cases} \quad (17)$$

Consequently, When increasing the boosting controller m , the chaotic signal x is boosted from a bipolar signal to a unipolar one as illustrated in Figure 11. The phase portraits in different planes and different values of the offset boosting controller m are given in Figures 10 and 12.

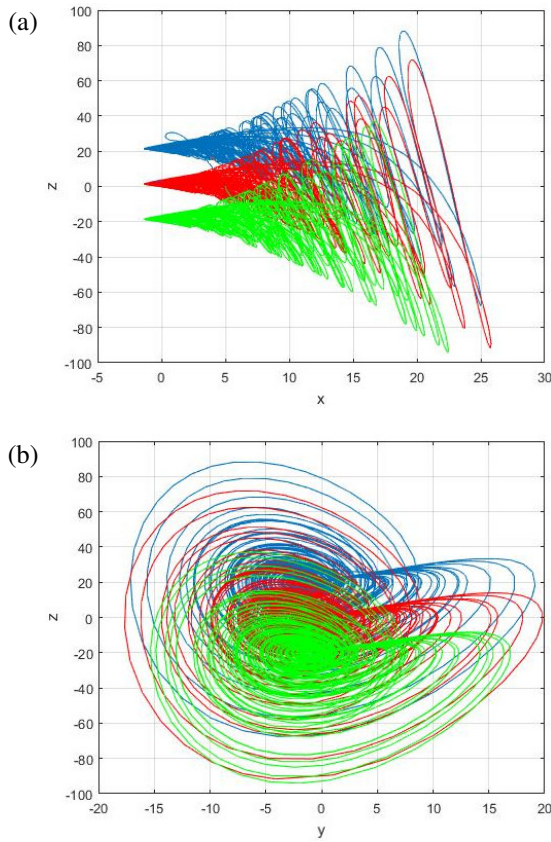


Figure 10: Phase portraits of the system (16) in different planes and different values of the offset boosting controller m : (a) $x - z$ plane, (b) $y - z$ plane for $m = -20$ (blue colour); $m = 0$ (red colour); $m = 20$ (green colour)

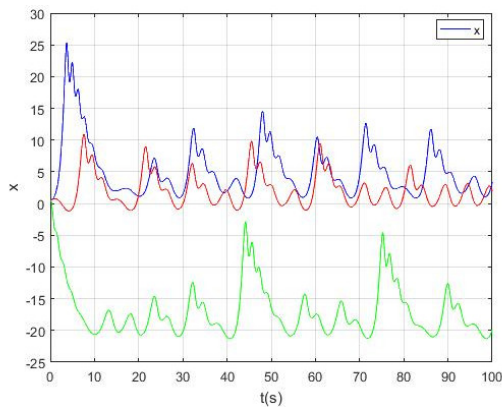


Figure 11: The signal x of the system (17) with different values of the offset boosting controller m : for $m = -2$ (blue colour); $m = 0$ (red colour); $m = 20$ (green colour)

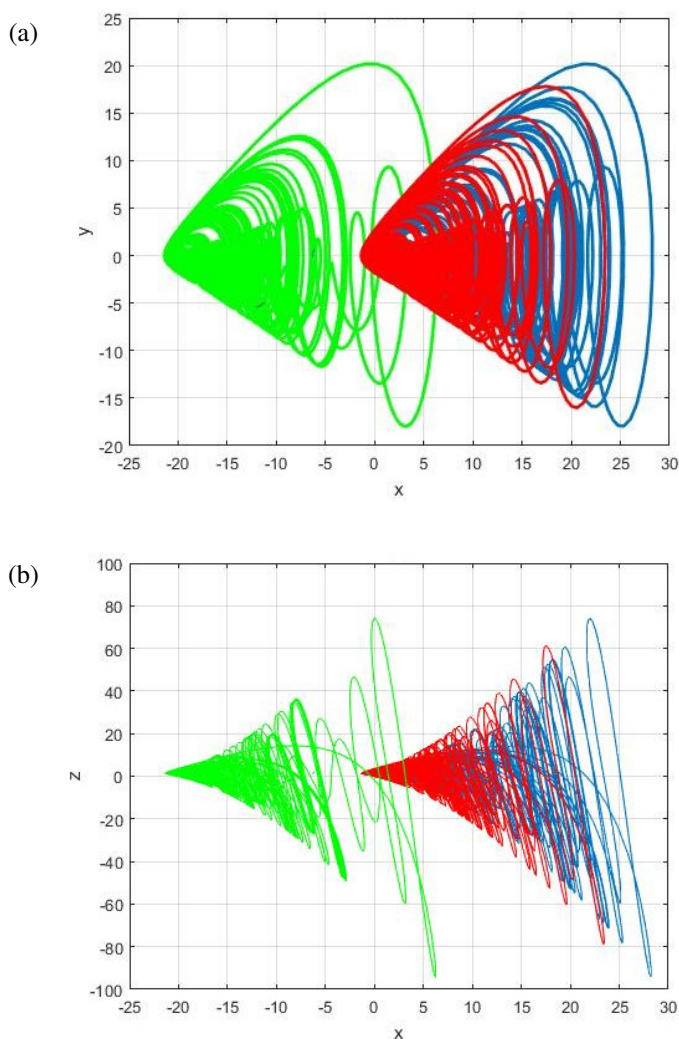


Figure 12: Phase portraits of the system (17) in different planes and different values of the offset boosting controller m : (a) $x - y$ plane, (b) $x - z$ plane for $m = -2$ (blue colour); $m = 0$ (red colour); $m = 20$ (green colour)

6. Circuit simulation of the new 3-D chaotic jerk system

In this section, the new 3D chaotic jerk system (3) is realized by the NI Multisim 14.1 platform. The electronic circuit design of the 3-D chaotic jerk system (3) is shown in Figure 13 in which TLO82CD is selected as OPAMP and the multipliers are of type AD633. Applying the Kirchhoff's laws, the circuit presented in Figure 13 is described by the following equations:

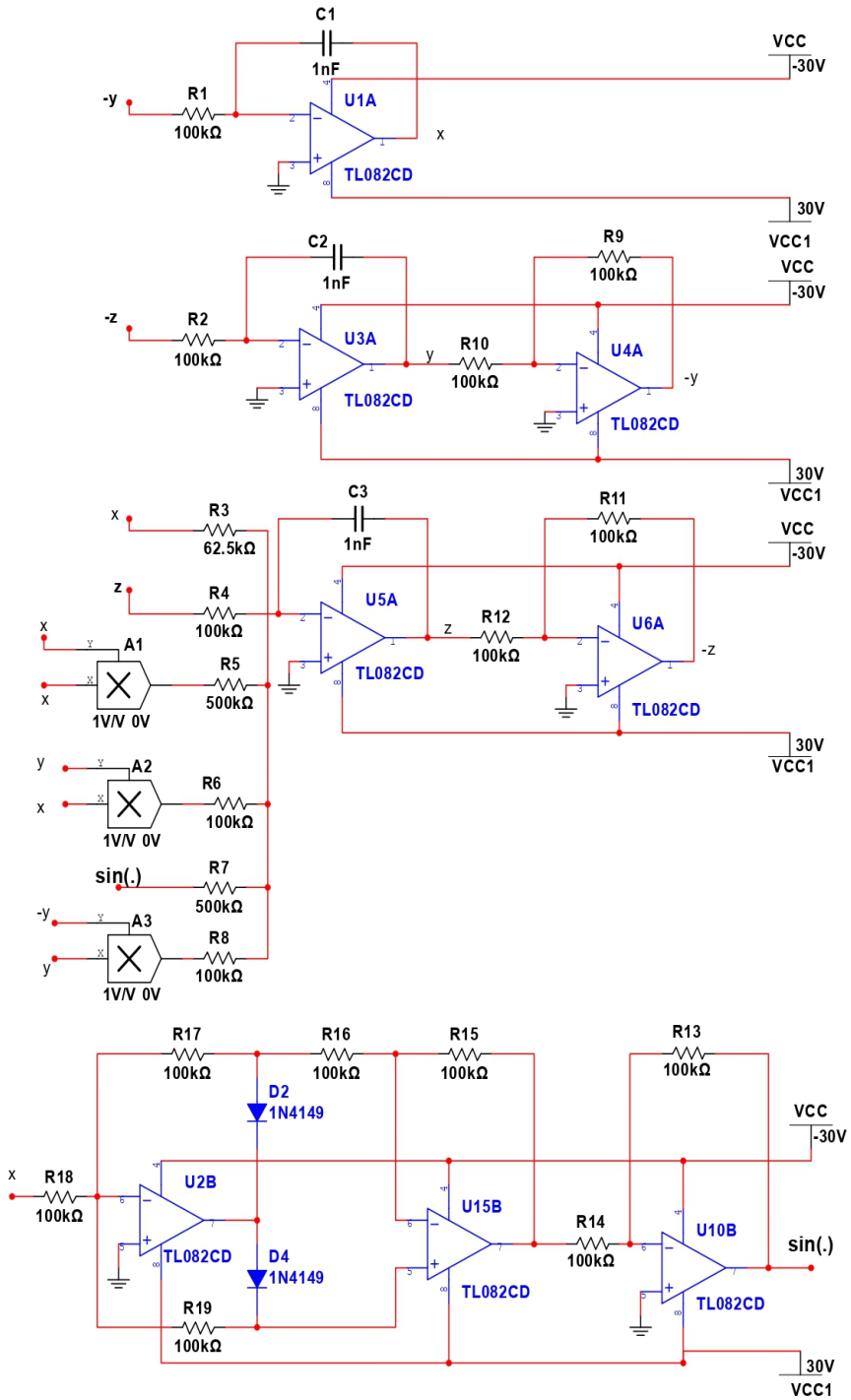


Figure 13: Circuit design of the new 3-D chaotic jerk system (18)

$$\begin{aligned} \dot{x} &= \frac{1}{R_1 C_1} y, & \dot{y} &= \frac{1}{R_2 C_2} z, \\ \dot{z} &= -\frac{1}{R_3 C_1} x - \frac{1}{R_8 C_3} \sin(x) - \frac{1}{R_6 C_3} (x)^2 - \frac{1}{R_7 C_3} xy + \frac{1}{R_9 C_3} (y)^2 - \frac{1}{R_5 C_3} z. \end{aligned} \quad (18)$$

Here x, y, z , are correspond to the voltages on the integrators U1A, U3A, U5A, respectively. The values of components in the circuit are selected as: $R_3 = 62.5 \text{ k}\Omega$, $R_5 = R_7 = 500 \text{ k}\Omega$, $R_1 = R_2 = R_4 = R_6 = 100 \text{ k}\Omega$, $R_i = 100 \text{ k}\Omega$, $i = 8, \dots, 19$. $C_1 = C_2 = C_3 = 1 \text{ nF}$. MultiSIM outputs of the circuit are presented in Figure 14.

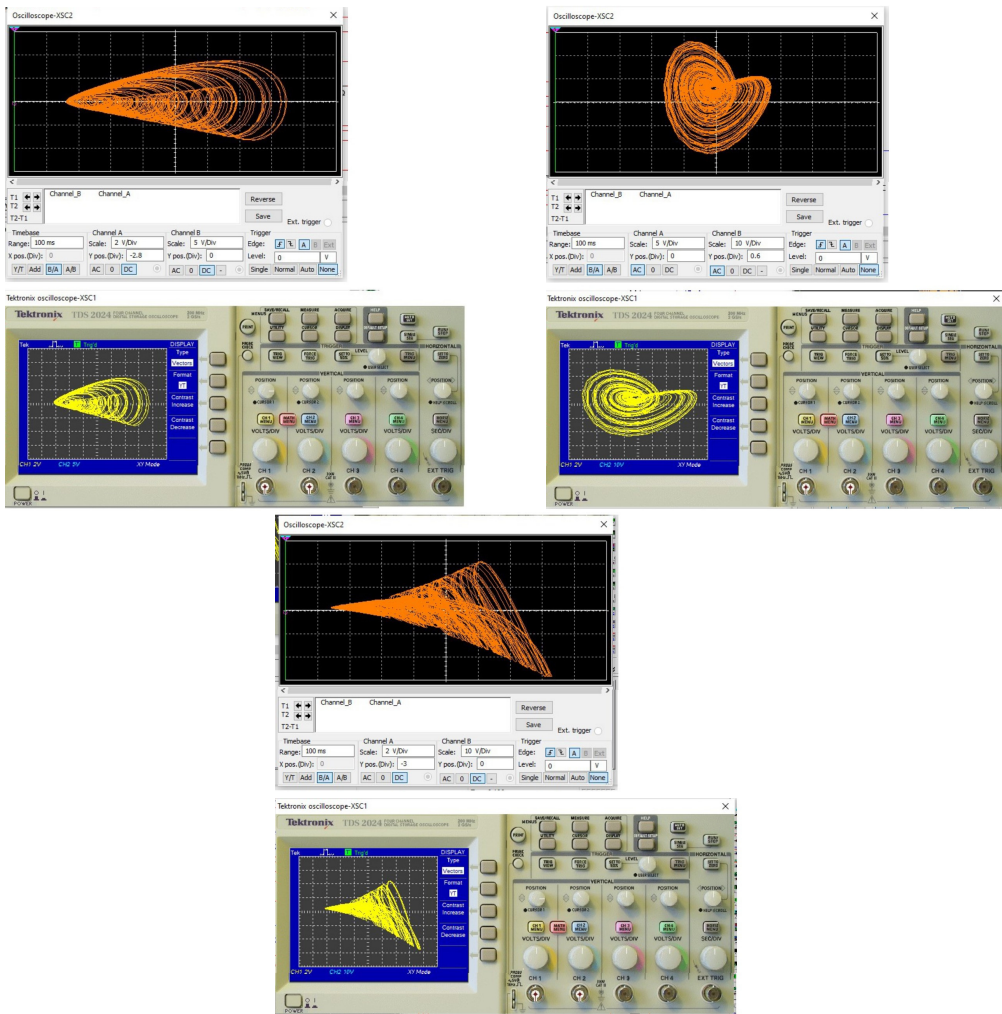


Figure 14: Chaotic attractors of the new 3D chaotic jerk circuit (18) via oscilloscope-XSC2 and Tektronix oscilloscope-XSC1

7. Complete synchronization of the new 3-D chaotic jerk systems

The mechanical jerk systems have a special triangular structure in their dynamics. In view of this special structure of the jerk systems, we apply the active backstepping control method [13] for the complete synchronization between the master and slave chaotic jerk systems. Synchronization of chaotic systems yields miscellaneous applications in secure communication systems [13].

The master and slave systems used for the synchronization can be compactly described as follows:

$$\begin{cases} \dot{x}_m = y_m, \\ \dot{y}_m = z_m, \\ \dot{z}_m = -ax_m - b \sin x_m - cx_m^2 + y_m^2 - x_my_m - z_m, \end{cases} \tag{19}$$

$$\begin{cases} \dot{x}_s = y_s, \\ \dot{y}_s = z_s, \\ \dot{z}_s = -ax_s - b \sin x_s - cx_s^2 + y_s^2 - x_sy_s - z_s + v. \end{cases} \tag{20}$$

Here, v is an active backstepping control, which is to be designed so as to achieve complete synchronization between the systems (19) and (20).

The synchronization errors between the jerk systems (19) and (20) can be defined as follows:

$$\begin{cases} \epsilon_x = x_s - x_m, \\ \epsilon_y = y_s - y_m, \\ \epsilon_z = z_s - z_m. \end{cases} \tag{21}$$

The error dynamics can be derived using a simple calculation as follows:

$$\begin{cases} \dot{\epsilon}_x = \epsilon_y, \\ \dot{\epsilon}_y = \epsilon_z, \\ \dot{\epsilon}_z = -a\epsilon_x - \epsilon_z - b(\sin x_s - \sin x_m) - c(x_s^2 - x_m^2) - x_sy_s + x_my_m + v. \end{cases} \tag{22}$$

The main control result of this section can be stated as follows:

Theorem 1. *The active backstepping control law defined by the equation*

$$v = -(3-a)\epsilon_x - 5\epsilon_y - 2\epsilon_z + b(\sin x_s - \sin x_m) + c(x_s^2 - x_m^2) + x_sy_s - x_my_m - ZW_3 \tag{23}$$

with the feedback gain $Z > 0$ and $w_3 = 2\epsilon_x + 2\epsilon_y + \epsilon_z$ achieves complete exponential synchronization between the chaotic jerk systems (19) and (20) for all initial states in \mathbb{R}^3 .

Proof. We begin with the Lyapunov function

$$V_1(w_1) = \frac{1}{2} w_1^2, \quad (24)$$

where

$$w_1 = \epsilon_x. \quad (25)$$

Then we get

$$\dot{W}_1 = w_1 \dot{w}_1 = \epsilon_x \epsilon_y = -w_1^2 + w_1(\epsilon_x + \epsilon_y). \quad (26)$$

Next, we define

$$w_2 = \epsilon_x + \epsilon_y \quad (27)$$

Then Eq. (26) reduces to

$$\dot{V}_1 = -w_1^2 + w_1 w_2 \quad (28)$$

Next, we define the candidate Lyapunov function

$$V_2(w_1, w_2) = V_1(w_1) + \frac{1}{2} w_2^2 = \frac{1}{2} w_1^2 + \frac{1}{2} w_2^2. \quad (29)$$

We find that

$$\dot{V}_2 = -w_1^2 - w_2^2 + w_2(2\epsilon_x + 2\epsilon_y + \epsilon_z). \quad (30)$$

To simplify the notations, we set

$$w_3 = 2\epsilon_x + 2\epsilon_y + \epsilon_z. \quad (31)$$

Then Eq. (30) reduces to

$$\dot{W}_2 = -w_1^2 - w_2^2 + w_2 w_3. \quad (32)$$

As a final step of the backstepping control design, we consider the candidate Lyapunov function

$$V(w_1, w_2, w_3) = V_2(w_1, w_2) + \frac{1}{2} w_3^2. \quad (33)$$

It is easy to see that V is a quadratic and positive definite function on \mathbb{R}^3 .

It is easy to realize that

$$V(w_1, w_2, w_3) = \frac{1}{2} w_1^2 + \frac{1}{2} w_2^2 + \frac{1}{2} w_3^2. \quad (34)$$

Calculating the derivative of V , we find that

$$\dot{V} = -w_1^2 - w_2^2 - w_3^2 + w_3 S, \quad (35)$$

where

$$S = w_2 + w_3 + \dot{w}_3. \quad (36)$$

A simple calculation shows that

$$S = (3 - a)\epsilon_x + 5\epsilon_y + 2\epsilon_z - b(\sin x_s - \sin x_m) - c(x_s^2 - x_m^2) - x_s y_s + x_m y_m + v. \quad (37)$$

Substituting the formula given in Eq. (23) for v into Eq. (36), we get

$$S = -Zw_3. \quad (38)$$

From the equations (35) and (38), we get

$$\dot{V} = -w_1^2 - w_2^2 - w_3^2(1 + Z). \quad (39)$$

Since $Z > 0$, we see that \dot{V} is a quadratic and negative definite function defined on \mathbb{R}^3 .

By Lyapunov Stability Theory, we deduce that the error dynamics (22) is globally exponentially stable.

For MATLAB simulations, we pick the parameters of the master and slave chaotic jerk systems as follows: $a = 1.6$, $b = 0.2$ and $c = 0.2$. Also, we take $Z = 30$.

For simulations, the initial conditions of the master system (19) are taken as $x_m(0) = 5.2$, $y_m(0) = 1.8$ and $z_m(0) = 4.9$.

Also, the initial condition of the slave system (20) are taken as $x_s(0) = 1.7$, $y_s(0) = 9.5$ and $z_s(0) = 2.4$.

Figure 15 shows the convergence of the synchronization errors ϵ_x , ϵ_y and ϵ_z between the chaotic jerk systems (19) and (20).

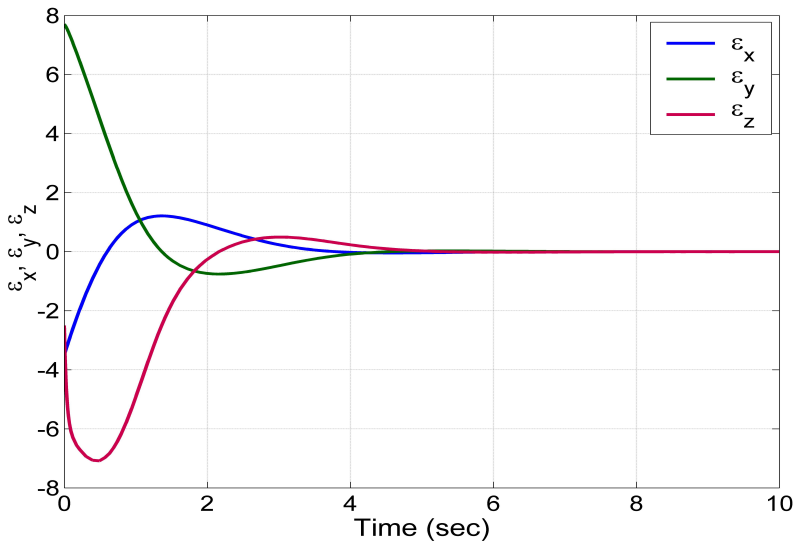


Figure 15: MATLAB plot depicting the exponential convergence of the complete synchronization error between the chaotic jerk systems (19) and (20)

8. Conclusions

In this research work, we contributed a new three-dimensional jerk system with three parameters in which one of the nonlinear terms is a sinusoidal nonlinearity. We showed that the new jerk system has two unstable equilibrium points on the x -axis. We carried out a detailed bifurcation analysis on the proposed chaotic jerk system. Using numerical integrations, we showed the existence of periodic and chaotic states, as well as unbounded solutions. Consideration of the Poincaré sphere at infinity found no periodic states. We showed that the new jerk system exhibits multistability with coexisting attractors. We also discussed results for the offset boosting of the proposed chaotic jerk system. Using MultiSim version 14.1, we designed an electronic circuit for the new jerk system with a sinusoidal nonlinearity. As a control application, we designed complete synchronization for the master-slave jerk systems using backstepping control technique. Simulations were shown to illustrate the main results of this research work.

References

- [1] D. DING, W. WANG, Z. YANG, Y. HI, J. WANG, M. WANG, Y. NIU and H. ZHU: An n -dimensional modulo chaotic system with expected Lyapunov exponents and its application in image encryption. *Chaos, Solitons & Fractals*, **174** (2023). DOI: [10.1016/j.chaos.2023.113841](https://doi.org/10.1016/j.chaos.2023.113841)
- [2] S. SAHOO and B.K. ROY: Design of multi-wing chaotic systems with higher largest Lyapunov exponent. *Chaos, Solitons & Fractals*, **157** (2022). DOI: [10.1016/j.chaos.2022.111926](https://doi.org/10.1016/j.chaos.2022.111926)
- [3] E. GOKCAY and H. TORA: A novel data encryption method using an interlaced chaotic transform. *Expert Systems with Applications*, **237** (2024). DOI: [10.1016/j.eswa.2023.121494](https://doi.org/10.1016/j.eswa.2023.121494)
- [4] H. WEN and Y. LIN: Cryptanalysis of an image encryption algorithm using quantum chaotic map and DNA coding. *Expert Systems with Applications*, **237** (2024). DOI: [10.1016/j.optlastec.2017.04.022](https://doi.org/10.1016/j.optlastec.2017.04.022)
- [5] Q. LAI and H. ZHANG: A new image encryption method based on memristive hyperchaos. *Optics and Laser Technology*, **166** (2023). DOI: [10.1016/j.optlastec.2023.109626](https://doi.org/10.1016/j.optlastec.2023.109626)
- [6] S. YAN, Y. ZHANG, Y. REN, X. SUN, Y. CUI and L. LI: A new locally active memristor and its chaotic system with infinite nested coexisting attractors. *Nonlinear Dynamics*, **111**(18), (2023), 17547–17560. DOI: [10.1007/s11071-023-08731-0](https://doi.org/10.1007/s11071-023-08731-0)
- [7] A.L.O. DUARTE and M. EISENCRAFT: Denoising of discrete-time chaotic signals using echo state networks. *Signal Processing*, **214** (2024). DOI: [10.1016/j.sigpro.2023.109252](https://doi.org/10.1016/j.sigpro.2023.109252)
- [8] D. CHEN, S. SHI and X. GU: Chaos detection scheme for multiple variable-frequency signals with overlapping frequencies. *Eurasip Journal on Advances in Signal Processing*, **2023**(1), (2023). DOI: [10.1186/s13634-023-01050-x](https://doi.org/10.1186/s13634-023-01050-x)
- [9] H.E. KIRAN, A. AKGUL, O. YILDIZ and E. DENIZ: Lightweight encryption mechanism with discrete-time chaotic maps for internet of robotic things. *Integration*, **93** (2023). DOI: [10.1016/j.vlsi.2023.06.001](https://doi.org/10.1016/j.vlsi.2023.06.001)

- [10] E. PETAVRATZIS, C. VOLOS and I. STOUBOULOS: Experimental study of terrain coverage of an autonomous chaotic mobile robot. *Integration*, **90** (2023), 104–114. DOI: [10.1016/j.vlsi.2023.01.010](https://doi.org/10.1016/j.vlsi.2023.01.010)
- [11] S.S. ALZAID, A. KUMAR, S. KUMAR and B.S.T. ALKAHTANI: Chaotic behavior of financial dynamical system with generalized fractional operator. *Fractals*, **31**(4), (2023). DOI: [10.1142/S0218348X2340056X](https://doi.org/10.1142/S0218348X2340056X)
- [12] A. AZAM and D.A. SUNNY: Generation of multiscroll chaotic attractors of a finance system with mirror symmetry. *Soft Computing*, **27**(6), (2023), 2769–2782. DOI: [10.1007/s00500-022-07501-1](https://doi.org/10.1007/s00500-022-07501-1)
- [13] S. VAIDYANATHAN and A.T. AZAR: *Backstepping Control of Nonlinear Dynamical Systems*. Academic Press, London, U.K., 2021.
- [14] S. VAIDYANTHAN, A.S.T. KAMMOGNE, E. TLELO-CUAUTLE, C.N. TALONANG, B. ABD-EL-ATTY, A.A. ABD EL-LATIF, E.M. KENGNE, V.F. MAWAMBA, A. SAMBAS, P. DARWIN and B. OVILLA-MARTINEZ: A novel 3-D jerk system, its bifurcation analysis, electronic circuit design and a cryptographic application. *Electronics*, **12**(13), (2023). DOI: [10.3390/electronics12132818](https://doi.org/10.3390/electronics12132818)
- [15] F. LI and J. ZENG: Multi-scroll attractor and multi-stable dynamics of a three-dimensional jerk system. *Energies*, **16**(5), (2023). DOI: [10.3390/en16052494](https://doi.org/10.3390/en16052494)
- [16] Y. XIA, S. HUA and Q. BI: Quasi-periodic structure in chaotic bursting attractor for a controlled jerk oscillator. *Chaos, Solitons & Fractals*, textbf174 (2023). DOI: [10.1016/j.chaos.2023.113902](https://doi.org/10.1016/j.chaos.2023.113902)
- [17] S. VAIDYANATHAN, E. TLELO-CUAUTLE, K. BENKOUIDER, A. SAMBAS and B. OVILLA-MARTINEZ: FPGA-based implementation of a new 3-D multistable chaotic jerk system with two unstable balance points. *Technologies*, **11**(4), (2023). DOI: [10.3390/technologies11040092](https://doi.org/10.3390/technologies11040092)
- [18] K. ZOURMBA, C. FISCHER, B. GAMBO, J.Y. EFFA and A. MOHAMADOU: Chaotic oscillator with diode-inductor nonlinear bipole-based jerk circuit: Dynamical study and synchronization. *Journal of Circuits, Systems and Computers*, **32**(12), (2023). DOI: [10.1142/S0218126623502146](https://doi.org/10.1142/S0218126623502146)
- [19] J. LI and N. CUI: Dynamical analysis of a new 5D hyperchaotic system. *Physica Scripta*, **98**(10), (2023). DOI: [10.1088/1402-4896/acf41a](https://doi.org/10.1088/1402-4896/acf41a)
- [20] H. WANG, G. KE, J. PAN and Q. SU: Modeling, dynamical analysis and numerical simulation of a new 3D cubic Lorenz-like system. *Scientific Reports*, **13**(1), (2023). DOI: [10.1038/s41598-023-33826-4](https://doi.org/10.1038/s41598-023-33826-4)
- [21] L. LASKARIDIS, C. VOLOS, H. NISTAZAKIS and E. MELETLIDOU: Exploring the dynamics of a multistable general model of discrete memristor-based map featuring an exponentially varying memristance. *Integration*, **95** (2024). DOI: [10.1016/j.vlsi.2023.102131](https://doi.org/10.1016/j.vlsi.2023.102131)
- [22] F. YU, Y. YUAN, C. WU, W. YAO, C. XU, S. CAI and C. WANG: Modeling and hardware implementation of a class of Hamiltonian conservative chaotic systems with transient quasi-period and multistability. *Nonlinear Dynamics*, **112**(3), (2024), 2331–2347. DOI: [10.1007/s11071-023-09148-5](https://doi.org/10.1007/s11071-023-09148-5)

- [23] C. LI, Y. JIANG and X. MA: On offset boosting in chaotic system. *Chaos*, **3**(2), (2021), 47–54. DOI: [10.51537/chaos.959841](https://doi.org/10.51537/chaos.959841)
- [24] X. ZHANG, J. XU and A.J. MOSHAYEDI: Design and FPGA implementation of a hyperchaotic conservative circuit with initial offset-boosting and transient transition behavior based on memcapacitor. *Chaos, Solitons and Fractals*, **179** (2024). DOI: [10.1016/j.chaos.2024.114460](https://doi.org/10.1016/j.chaos.2024.114460)
- [25] J. ZHANG, Y. GUO and J. CUO: Design of memristor hyperchaotic circuit with burst oscillation and infinite attractor coexistence and its application. *Microelectronic Engineering*, **282** (2023). DOI: [10.1016/j.mee.2023.112099](https://doi.org/10.1016/j.mee.2023.112099)
- [26] A. DLAMINI and E.F. DOUNGMO GOUFO: Generation of self-similarity in a chaotic system of attractors with many scrolls and their circuit's implementation. *Chaos, Solitons & Fractals*, **176** (2023). DOI: [10.1016/j.chaos.2023.114084](https://doi.org/10.1016/j.chaos.2023.114084)
- [27] T. BONNY, W.A. NASSAN, S. VAIDYANATHAN and A. SAMBAS: Highly-secured chaos-based communication system using cascaded masking technique and adaptive synchronization. *Multimedia Tools and Applications*, **82**(22), (2023). DOI: [10.1007/s11042-023-14643-3](https://doi.org/10.1007/s11042-023-14643-3)
- [28] S. VAIDYANATHAN and A.T. AZAR: Adaptive control and synchronization of Halvorsen circulant chaotic systems. *Studies in Fuzziness and Soft Computing*, **337** (2016), 225–247. DOI: [10.1007/978-3-319-30340-6_10](https://doi.org/10.1007/978-3-319-30340-6_10)
- [29] N. DEBDOUCHE, L. ZAROUR, H. BENHOUEHNI, F. MEHAZZEM and B. DEFFAF: Robust integral backstepping control microgrid connected photovoltaic System with battery energy storage through multi-functional voltage source inverter using direct power control SVM strategies. *Energy Reports*, **10** (2023), 565–580. DOI: [10.1016/j.egy.2023.07.012](https://doi.org/10.1016/j.egy.2023.07.012)
- [30] J.D. BARROS, L. ROCHA and J.F. SILVA: Backstepping control of NPC multilevel converter interfacing AC and DC microgrids. *Energies*, **16**(14), (2023). DOI: [10.3390/en16145515](https://doi.org/10.3390/en16145515)
- [31] E. ÖZALP, G. MARGAZOGLU and L. MAGRI: Reconstruction, forecasting, and stability of chaotic dynamics from partial data. *Chaos*, **33**(9), (2023). DOI: [10.1063/5.0159479](https://doi.org/10.1063/5.0159479)